

## Crystalline Structure and Physical Properties of High-Entropy Film Alloys

Yu.S. Bereznyak<sup>1</sup>, M. Opielak<sup>2</sup>, L.V. Odnodvoretz<sup>1</sup>, D.V. Poduremne<sup>1</sup>, I.Yu. Protsenko<sup>1,\*</sup>, Yu.M. Shabelnyk<sup>1</sup>

<sup>1</sup> Sumy State University, 2, Rymyskyi-Korsakov Str., 40007 Sumy, Ukraine  
<sup>2</sup> Lublin University of Technology, 38A, Nadbystrzycka Str., 20-618 Lublin, Poland

(Received 12 November 2018; revised manuscript received 04 April 2019; published online 15 April 2019)

The results of the study of phase composition, electrophysical (resistivity, thermal coefficient of resistance), magnetoresistivity (giant magnetoresistance) and magnetic (magnetization) properties of thin films (up to 100 nm) of high-entropy alloys based on Al, Cu, Ni, Fe and Co are presented. It was established that after the formation of samples by layered deposition on diffraction pattern, lines from two phases with a fcc lattice and traces of the bcc phase are fixed. After homogenization by thermal annealing of the samples, there remains one fcc phase s.s. HEA ( $\alpha = 0.360-0.365$  nm) and traces of the bcc phase (most likely s.s.  $\alpha$ -Fe(Cr)), that is, in fact, single-phase. It was received that the dependence of the magnetoresistance versus induction has all the features of the GMR with amplitude 0.15-0.20 %. Resistivity and thermal coefficient of resistance have relatively large values  $\rho \sim 10^{-7}$  Ohm.m and  $\beta \sim 10^{-3}$  K<sup>-1</sup>. Within the size effect models in the temperature coefficient of resistance, the mean free path of electrons ( $\lambda = 73-85$  nm) is calculated. The field and temperature dependences of the magnetization at the magnetic field induction  $B = 0.5$  T ( $T = 2$  and 300 K) at the conditions field of cooling (FC) and cooling without a magnetic field (ZFC) in the temperatures range from 2 to 400 K are presented.

**Keywords:** High-entropy alloy, Elemental composition, Resistivity, Temperature coefficient of resistance, Magnetoresistance, Magnetization.

DOI: [10.21272/jnep.11\(2\).02026](https://doi.org/10.21272/jnep.11(2).02026)

PACS numbers: 61.66.Xx, 62.20.F-, 75.47.Np

### 1. INTRODUCTION

In recent years, intensive studies of the crystalline structure, mechanical and magnetic properties of a new class of materials - high-entropy alloys (HEA) [1-4] in the form of bulk samples based on ferromagnetic (Fe, Ni, Co), fcc (Al, Cu etc.), bcc (Cr, V) or hpc (Hf, Zr, Ti) metals have been carried out. HEA is classified according to their structure. Typical representatives of HEA are the solid solutions (s.s.) based on Mo, Nb, Ta, W and V. Formation of the hcc structure is characteristic for HEA based on Co, Fe, Ni, Cr and Cu. HEA based on Co, Ti, Zr with hpc structure is less common.

The conditions for the formation of equiatomic HEA there are values (see, for example, [5]):

$$- \text{mixing entropy } \Delta S_{mix} = -R \sum_{(i)} c_i \ln c_i \geq 1.61R \text{ (for}$$

five and more components);

$$- \text{empirical parameter of difference of atomic sizes}$$

$$\delta = \sqrt{\sum_{i=1}^n c_i \left(1 - \frac{r_i}{\bar{r}}\right)^2} \leq 5\%;$$

$$- \text{enthalpy mixing of multicomponent solid solution}$$

$$\Delta H_{mix} = \sum_{(i, j \neq i)} 4\Delta H_{ijmix} c_i c_j,$$

where  $r_i$  – the atomic radius  $i$ - element;

$c_i$  – the concentration  $i$ - component;

$\bar{r}$  – average atomic radius;

$\Delta H_{ijmix}$  – mixing enthalpy of two-component alloy equiatomic alloy. We note that the samples tested meet these conditions.

At the moment, considerable experimental material has been accumulated (see, for example, [5]) about

mechanical and magnetic properties of HEA in a bulk state. We have initiated the research [6, 7] of electro-physical properties (resistivity, thermal resistance – TCR) and magnetoresistive (giant magnetoresistance – GMR) properties based on Cu, Al, Cr, Fe, Ni and Co.

The purpose of this work was as in the subsequent study of electrophysical and magnetoresistive properties of multicomponent film alloys with different concentrations of magnetic components.

### 2. EXPERIMENT TECHNIQUE

The film samples are condensed with method layer by layer condensation with control the thickness of the individual layers by quartz resonator method. For the diffraction and electron-microscopic studies was used NaCl-substrate (S), and for the resistance and magnetoresistance measured and EDS spectra to obtain – ceramic substrate, to measure of magnetization and EDS spectra to obtain was used polysilicon with naturally oxidized superficial layer (SiO<sub>x</sub>).

On Fig.1 and Table 1 shows general characteristics of the samples and data on the chemical and elemental composition (QUANTA 600 FEG, firm «FEL», Netherlands) of the samples obtained by layer condensation, as well as experimental data on TCR are presented (see Section 3.2). On Fig. 2 shows the distribution maps of the elements.

The concentration of individual components was estimated by the ratio:

$$c_i = \frac{\rho_i d_i \mu_i^{-1}}{\sum_{i=1}^n \rho_i d_i \mu_i^{-1}},$$

where  $\rho_i$ ,  $d_i$  and  $\mu_i$  – density, thickness and molar mass of individual components, and refined by the method of energy-dispersion analysis.

\* [i.protsenko@aph.sumdu.edu.ua](mailto:i.protsenko@aph.sumdu.edu.ua)

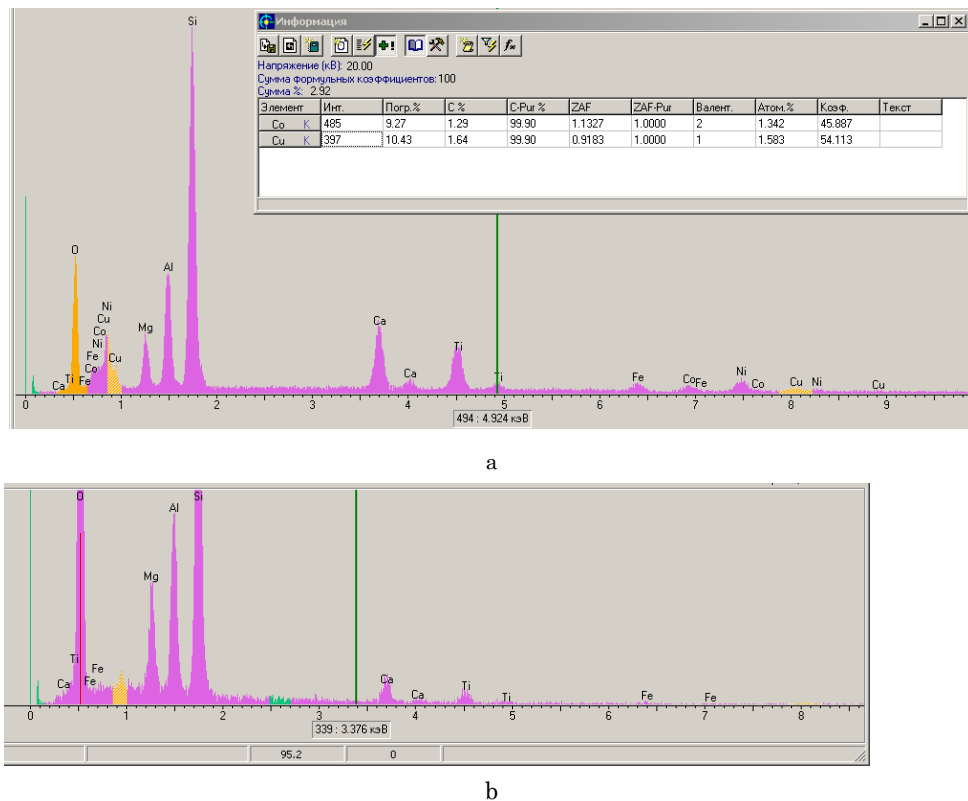


Fig. 1 – EDS spectra from Cu(5.5)/Ni(5.5)/Fe(5.5)/Co(5)/ Al(8)/S sample (a) and sital substrate (b)

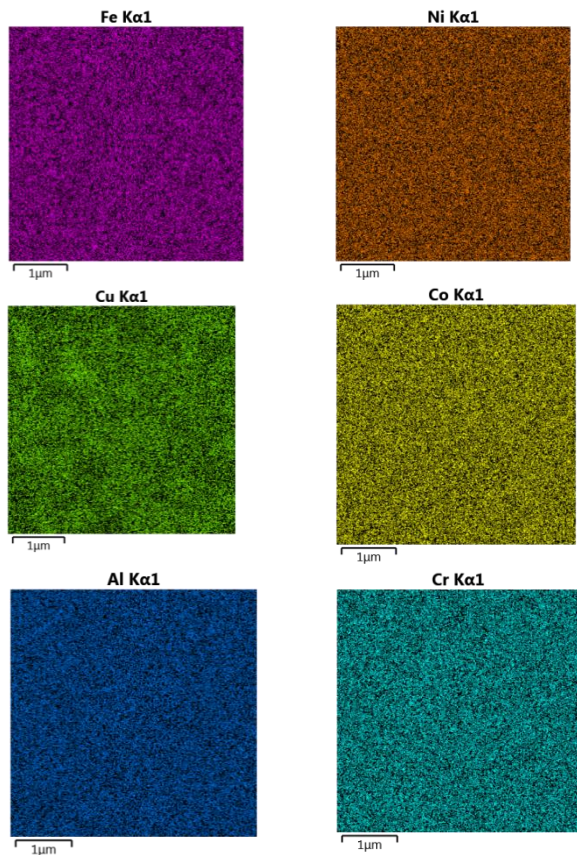


Fig. 2 – Map of elements distribution in sample Cr(7.5)/Al(4.5)/Co(7.3)/ Cu(4.8)/Ni(7)/Fe(7)/S

Structural and diffraction studies were held on device TEM-125K (firm Selmi, Sumy). Based on the temperature dependence of the resistivity ( $\rho$ ) (II temperature cycle at the cooling) calculated thermal coefficient of resistance (TCR) base on ratio  $\beta = \frac{\rho(T) - \rho(300)}{\rho(300)(T - 300)}$ . The value of magnetoresistance (MR) calculated based on field dependence  $R(B)$  by ratio  $MR = \frac{R(B_i) - R(0)}{R(0)}$ . To measure  $\rho(T)$  and  $R(B_i)$  and calculate TCR and MR used appropriate computerized complex.

Table 1 – General characteristic of HEA films

No	Sample (thickness, nm)	Concentration, at. %	TCR $10^3, K^{-1}$ at the $T = 300 K$
1	Fe(28)/Co(12)/Al(15)/Ni(17)/Cu(17)/S	30/15/12/21/21/S	3.00
2	Fe(18)/Co(12)/Al(15)/Ni(17)/Cu(17)/S	23/17/14/23/23/S	3.24
3	Fe(14)/Co(17)/Al(21)/Ni(15)/Cu(7)/S	20/26/21/23/10/S	2.57
4	Al(20)/Co(34)/Fe(32)/Ni(38)/Cu(31)/S	18/22/23/23/13/S	3,00
5	Al(4)/Cu(3.2)/Co(4.5)/Cr(5.2)/Fe(4.7)/S	11/13/19/20/19/17/11/S	2.00
6	Cr(7.5)/Al(4.5)/Co(7.3)/Cu(4.8)/Ni(7)/Fe(7)/S	19/8/21/12/19/19/S	1.80
7	Cu(5.5)/Ni(5.5)/Fe(5.5)/Co(5)/Al(8)/S	20/21/19/20/20/S	–
8	Co(20)/Ni(14)/Cu(19)/Fe(29)/Al(18)/S	22/15/20/30/13/S	–

The films magnetization was measured on a magnetometer MPMS3 (SQUID) in parallel and perpendicular orientation of the magnetic field relative to the sample plane.

3. RESULTS AND DISSCUSION

3.1 Crystalline Structure

In Fig. 1 shows examples of a typical diffraction pattern and microstructure of film samples in non-annealed and annealed to 800 K state. It should be noted that the samples No1 and No2, like the others in Table 1, have a non-equiatomical composition and a slightly different concentration of magnetic components. This is manifested in some differences microstructures both in the initial state and after annealing (Fig. 3).

Microparticles of dark contrast (we call them quasi-granules), in our opinion, have a magnetic nature and have an important role in electrophysical and magnetoresistive properties. Spin-dependent scattering of electrons, which is a prerequisite for the realization of giant magnetic resistance (GMR), can be realized on quasi-granules. We note that earlier in the paper [8] noted the stabilization of such entities (the authors call them micro-domains) in bulk HEA, as additional centers of conduction electron scattering.

Diffraction studies indicate that in the film HEA the main phases can be the fcc phase based on Cu with the parameter  $a = 0.3604-0.3650$  nm or axial Al at its excess in the alloy with  $a = 0.4016-0.4050$  nm.

In the first case, along with lines from the base fcc phase, traces of the phase with a lattice parameter  $\alpha$ -Fe or bcc Cr are observed, which is interpreted as a solid solution  $\alpha$ -Fe(Cr). Sometimes there are traces of another phase, which the authors [3] interpret as an intermetallic NiAl.

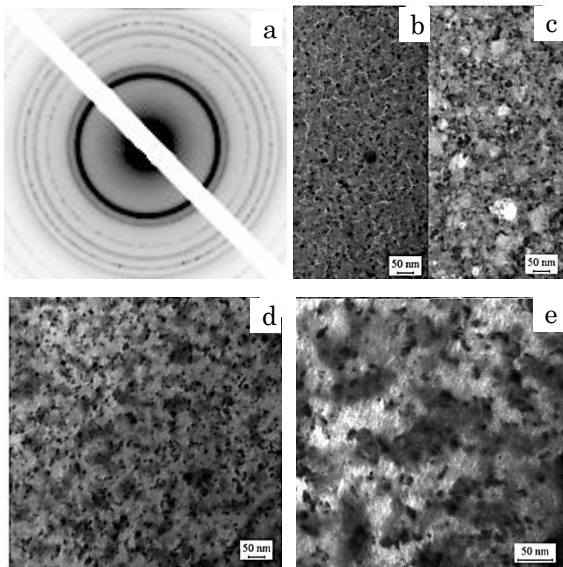


Fig. 3 – The diffraction pattern (a) and microstructure of sample No 1 (b, c) and film No 2 (d, e) as-deposition (a, b, d) and annealing to 800 K state (c, e)

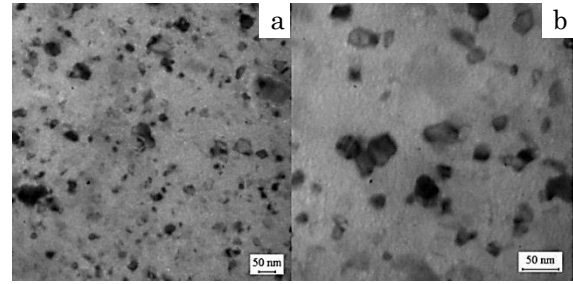


Fig. 4 – The microstructure of Fe(14)/Co(17)/Al(21)/Ni(15)/Cu(7)/S films as-deposition (a) and annealing to 800 K (b) states

3.2 Electrophysical Properties

Fig. 5 illustrates on the example of film No 2 the typical temperature dependence of resistivity ( $\rho$ ) and TCR ( $\beta$ ). The nonmonotonic nature of the dependence  $\rho(T)$  at the annealing is due to the processes of the atoms ordering and the healings of the crystalline structure defects. At cooling, there is a typical dependence  $\beta(T) \sim A/T$ . The TCR at the  $T = 300$  K varies within  $(1.8-3.0) \cdot 10^{-3} K^{-1}$  (Fig. 3, insert, Table 1).

Physical content  $A(T)$  becomes clear if you use the relations in the most general form for the resistivity

$$\rho(T) = BT^n + \rho_{res},$$

and temperature coefficient of resistance

$$\beta(T) = \frac{d \ln \rho}{dT}.$$

In a simpler form, when residual resistance  $\rho_{res} \ll \rho(T)$ ,  $\beta(T) = \frac{n}{T}$ , where indicator  $n = 1$  ( $\rho \sim T$ ),  $2$  ( $\rho \sim T^2$ ),  $3$  ( $\rho \sim T^3$ ) and, in the most common case  $0 < n \leq 5$ .

The results obtained by us can be compared only with data for bulk HEA, since there are no experimental data on the electrophysical properties of film alloys in the literature.

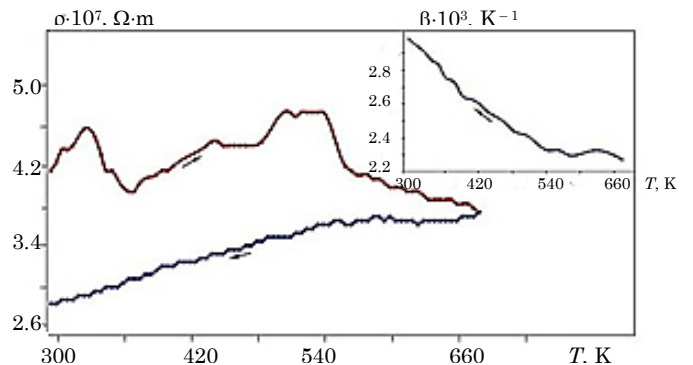


Fig. 5 – The temperature dependences of resistive and TCR (on insert) for HEA film Fe(28)/Co(12)/Al(15)/Ni(17)/Cu(17)/S.

An explanation of the large TCR is that the HEA has an unordered structure, which causes both a large  $\rho$  and its temperature sensitivity. Proceeding from the definition

$\beta = \frac{1}{\rho} \frac{\partial \rho}{\partial T}$ , it can be argued that a certain increase in the

value  $\rho$  is compensated by an increase  $\frac{\partial \rho}{\partial T}$ .

According to the data [8]  $\rho(300\text{ K})$  and  $\beta(300\text{ K})$  in bulk HEA based on Cr, Mn, Fe, Co and Ni the following values are  $0.11 \cdot 10^{-7}$  Ohm·m and  $0.35 \cdot 10^{-3} \text{ K}^{-1}$ , which an order of magnitude more in the case  $\rho$  and less in the case of  $\beta$  in comparison with our data. This can be explained by the high degree of disordered bulk HEA, as well as by slightly different elemental and phase composition.

Thus, the nonmonotonic dependence  $\rho(T)$  during annealing is not associated with any mechanisms of electron-phonon interaction. It reflects certain diffusion processes of atoms, which lead to the HEA ordering and the formation of the quasigranules.

Note that the calculation  $\beta(D)$  completely corresponds (Table 2) to the theoretical representation of the size effect in the TCR [9], since it has the same tendency to decrease the magnitude with increasing thickness, as in the case of single-layer films. Table 2 shows the results of TCR calculation based on the temperature dependence of the resistivity.

**Table 2** – Temperature coefficient of resistance for HEA films at the  $T = 300\text{ K}$

Sample (thickness, nm)	D, nm	$\beta \cdot 10^3, \text{ K}^{-1}$	$\beta \cdot D \cdot 10^2, \text{ nm} \cdot \text{K}^{-1}$
Fe(18)/Co(12)/Al(15)/Ni(17)/Cu(17)/S	80	3.24	25.9
Fe(22)/Co(17)/Al(12)/Ni(10)/Cu(13)/S	74	3.00	22.2
Fe(14)/Co(17)/Al(21)/Ni(15)/Cu(7)/S	74	2.57	19.0
Al(13)/Co(7)/Cu(5)/Ni(7)/Fe(7)/S	39	1.80	7.2
Al(4)/Cu(3)/Co(5)/Cr(5)/Fe(5)/S	22	2.00	-

We first attempted to estimate the TCR value under the condition  $D \rightarrow \infty$  and calculate the mean free path of conduction electrons in the HEA films. The calculations were performed within the framework of the Fuchs-Sondheimer model and using the linearized ratio by Tellier-Tosser-Pichard [9]. In the framework of these models, the dependence  $\beta(D)$  is rectified in the coordinates  $\beta \cdot D$  versus  $D$  (at the calculation not be the data for the last sample in Table 2 are taken into account, because it has a different chemical composition):

$$\beta \cdot D \square \beta_{\infty} \cdot D - \frac{3}{8} \lambda_{\infty} (1-p) \cdot \beta_{\infty}, \quad (\text{F-S})$$

$$\beta \cdot D \square \beta_g \cdot D - \lambda_g (1-p) \cdot \beta_g \cdot H(\alpha), \quad (\text{T-T-P})$$

where  $\beta_{\infty} = \lim_{D \rightarrow \infty} \beta$ ,  $\beta_g$  – TCR, which is due to the scattering of conduction electrons at the grain boundaries, defects of the crystalline structure and on phonons  $\beta_g \equiv \beta_{\infty}$ ;  $\lambda_g \equiv \lambda_{\infty}$  – the mean free path;  $p$  – the param-

eter of specular reflection from external surfaces of film;  $H(\alpha)$  – known function [9], which in our case  $\equiv 0.3$ .

As can be seen from the above equations, the angular coefficient of dependence  $\beta \cdot D$  versus  $D$  is  $\beta_{\infty}$  or  $\beta_g$ , and by the size of the segment that is cut off by the axis in, it is possible to calculate the value of the mean free path. The following results were obtained in a diffuse approximation (Table 3).

**Table 3** – Results of calculations

Model	$\beta, \text{ K}^{-1}$	$\lambda, \text{ nm}$	$p$	$H(\alpha)$
F-S	$3.5 \cdot 10^{-3}$	73	0	–
T-T-P	$3.5 \cdot 10^{-3}$	85	0	0.3

From the given values  $\lambda$ , it is more correct to consider  $\lambda = 85\text{ nm}$ , since the formula (T-T-P) partially takes into account grain boundary scattering of electrons through the parameter  $\alpha = \frac{\lambda}{L} \cdot \frac{R}{1-R}$ , where  $L$  is the average grain size,  $R$  – is the coefficient of electron scattering on the grain boundary.

The results we obtained for the mean free path of electrons can be compared with the data of work [10], which shows the dependence  $\lambda$  on the Al atoms concentration in a bulk high-entropy alloy Al<sub>x</sub>CoCrFeNi. At the  $T = 300\text{ K}$ , the value  $\lambda = 94\text{ nm}$  ( $x = 5.8\text{ at.}\%$ ) and decreases to  $\lambda = 60\text{ nm}$  ( $x = 15.8\text{ at.}\%$ ). In our case, the more precise value  $\lambda = 85\text{ nm}$  at the  $x = (8-21)\text{ at.}\%$  is well consistent with  $\lambda = 94\text{ nm}$ , which corresponds, as in our case, fcc alloy with traces of bcc-phase. We note that the alloys chemical composition in our case and the authors [10] is somewhat different.

Reasonable values  $\beta$  and  $\lambda$  once again confirm that the film HEA can be considered as single-layered multicomponent samples.

### 3.3 Magnetoresistance Properties

On Fig. 6 shows typical MR dependencies in three measurement geometries on an example of Co(20)/Ni(14)/Cu(19)/Fe(29)/Al(18)/S film. The amplitude of the MR in the range 0.15-0.17 % in three geometries of measurement and its field dependence suggest the realization of the GMR effect.

Such a situation is possible only in the case of spin-dependent scattering of electrons. We conclude that such scattering takes place on the quasigranules, since no other mechanism can be proposed. On Fig. 7 shows the temperature dependences of the magnetization for a sample Cu(5.5)/Ni(5.5)/Fe(5.5)/Co(5)/Al(8)/S.

We note that the film HEA has a relatively large coercivity force  $B_c \equiv 0.2\text{ T}$  (for comparison we note that according [10] in the alloy Al<sub>0.5</sub>CoCrFeNi (fcc + bcc) the value  $B_c \equiv 0.05\text{ mT}$ ). Such a distinction can be explained by different chemical composition of alloys. It should be noted that similar temperature dependences of FC and ZFC were observed by the authors [11] on the example of low-entropy alloy Cu<sub>0.47</sub>Co<sub>0.53</sub>.

The dependence  $M(T)$  under ZFC has a typical character for ferromagnets, when based on large-domains formed magnet-disordered range of permanent magnetization, which causes a slow reduction  $M$  to zero.

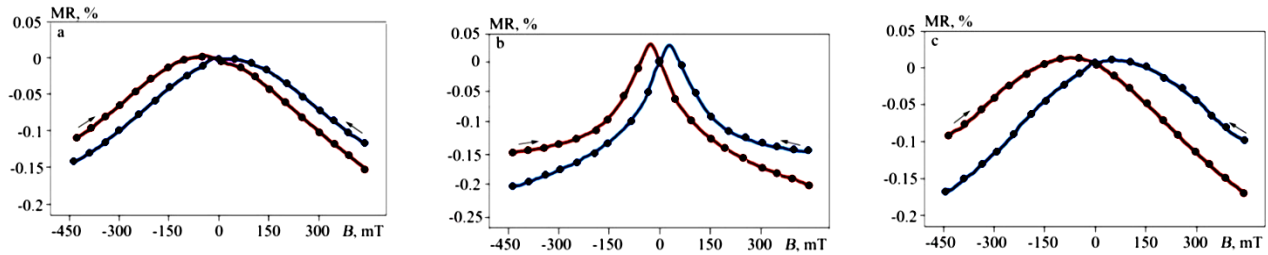


**Fig. 6** – Field dependence of MR for film HEA Co(20)/Ni(14)/Cu(19)/Fe(29)/Al(18)/S after annealing to 810 K for three geometries of measurement – longitudinal (a), perpendicular (b) and transverse (c), respectively. The arrows indicate the directions of magnetization – demagnetization

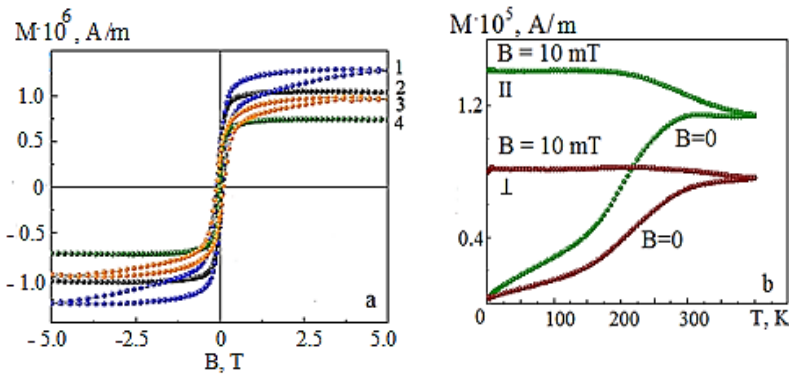


**Fig. 7** – Temperature dependence of the magnetization for a sample Cu(5.5)/Ni(5.5)/Fe(5.5)/Co(5)/Al(8)/S in parallel (1, 2) and perpendicular (3, 4) orientation of the magnetic field to the sample plane. Temperature: 1,3 – 300K; 2,4 – 2K (a) and the temperature dependence of the magnetization under the conditions FC ( $B = 10$  mT) and ZFC ( $B = 0$ ) in two geometrical measurements

#### 4. CONCLUSIONS

Investigations of the structural and phase state, electrophysical and magnetoresistive properties allow the following conclusions:

- at the layer-condensation of ultra thin layers (up to 30 nm) with subsequent annealing up to 800 K, it is possible to form a homogeneous HEA films with a fcc lattice and parameters close to the parameters of the excess component Cu or Al;
- resistivity and TCR have relatively high values. what can be explained by the film defects and the additional scattering of conduction electrons by magnetic quasi-granules;
- the mean free path of electrons  $\lambda = 73$  nm (Fuchs-Sondheimer model) and 85 nm (Tellier-Tosser-Pichard model) were calculated, which qualitatively agrees with the  $\lambda$  for analogous to the chemical composition of the HEA;

#### REFERENCES

1. J.W. Yeh, S.K. Chen, S.J. Lin, J.-Y. Gan, T.-S. Chin, T.-T. Shun, C.-H. Tsau, S.-Y. Chang, *Adv. Eng. Mater.* **6**(5), 299 (2004).
2. Y. Zhang, Y. Zhou, *Mater. Sci. Forum* **561-565**, 1337 (2007).
3. Yan Ping Wang, Bang Sheng Li, Heng Zhi Fu, *Adv. Eng. Mater.* **11**(8), 641 (2009).
4. Y. Zhang, T.T. Zuo, Y.Q. Cheng, P.K. Liaw, *Sci. Rep.* **3**, 1455 (2013).
5. Y.F. Ye, Q. Wang, J. Lu, C.T. Liu, Y. Yang, *Mater. Today* **19**(6), 349 (2016).
6. S.I. Vorobiov, D.M. Kondrakhova, S.A. Nepijko, D.V. Poduremne, N.I. Shumakova, I.Yu. Protsenko, *J. Nano-Electron. Phys.* **8**(3), 03026 (2016).
7. Yu.S. Bereznyak, L.V. Odnovorets, D.V. Poduremne, I.Yu. Protsenko, Yu.M. Shabelnyk, *High-entropy film alloys: Electrophysical and magnetoresistive properties* – 17 (Chapter in Book, Nanooptics, Nanophotonics, Nanostructures, and Their Applications: Springer: 2018).
8. Yu.P. Mazur, R.V. Ostapenko, M.P. Semen'ko, *Ukr. J. Phys.* **62**(5), 413 (2017).
9. C.R. Tiller, A.J. Tosser, *Size Effects in Thin Films* (Elsevier: 1982).
10. Y.-F. Kao, S.-K. Chen, T.-J. Chen, P.-C. Chu, J.-W. Yeh, S.-J. Lin, *J. Alloy. Compd.* **509**, 1607 (2011).
11. S.K. Ghosh, A. Dogra, C. Srivastava, S.K. Gupta, *J. Alloy. Compd.* **504**, 452 (2010).

- the dependence of MR versus magnetic field induction has all the characteristics of the GMR, which makes it possible to conclude that spin-dependent electron scattering;

- the field dependences ( $B = 0-5$  T) of the magnetization at the  $T = 2$  and 300 K and the temperature ( $T = 2-400$  K) dependences at the conditions FC ( $B = 10$  mT) and ZFC are obtained.

The authors express their gratitude to D.A. Kolesnikov for received the EDS spectra and S.I. Vorobiov for help in conducting magnetic research.

The work was performed with Ministry of Education and Science of Ukraine financial support (grant No 2018-2020 years).

**Кристалічна структура і фізичні властивості високоентропійних сплавів**Ю.С. Березняк<sup>1</sup>, М. Оpielak<sup>2</sup>, Л.В. Однодворець<sup>1</sup>, Д.В. Подуремне<sup>1</sup>, І.Ю. Проценко<sup>1</sup>, Ю.М. Шабельник<sup>1</sup><sup>1</sup> Сумський державний університет, вул. Римського-Корсакова, 2, 40007 Суми, Україна<sup>2</sup> Lublin University of Technology, 38A, Nadbystrzycka Str., 20-618 Lublin, Poland

Представлені результати дослідження фазового складу, електрофізичних (опір, температурний коефіцієнт опору), магніторезистивних (гігантський магнітоопір) та магнітних (намагніченість) властивостей тонких високоентропійних плівкових (до 100 нм) сплавів на основі Al, Cu, Ni, Fe та Co. Встановлено, що після формування зразків методом пошарової конденсації на дифракційній картині фіксуються лінії від двох фаз з ГЦК-решіткою та сліди ОЦК-фази. Після гомогенізації шляхом термічного відпалювання зразків залишається одна ГЦК-фаза т.р. HEA ( $a = 0,360-0,365$  нм) і сліди ОЦК-фази (швидше за все, s.s.  $\alpha$ -Fe(Cr)), тобто плівки стають фактично однофазними. Отримано, що залежність магнітоопору від індукції має ознаки ГМО з амплітудою 0,15-0,20 %. Величини питомого опору і термічного коефіцієнту опору мають відносно великі значення  $\rho \sim 10^{-7}$  Ом·м і  $\beta \sim 10^{-3}$  К<sup>-1</sup>. У рамках моделей розмірного ефекту в термічному коефіцієнті опору розрахована величина середньої довжини вільного пробігу електронів ( $\lambda = 73-85$  нм). Представлені польові і температурні залежності намагніченості в інтервалах індукції магнітного поля  $B = 0-5$  Т ( $T = 2$  і 300К) при польовому охолодженні (FC) і охолодженні без дії магнітного поля (ZFC) в інтервалі температур 2-400 К.

**Ключові слова:** Високоентропійний сплав, Елементарний склад, Питомий опір, Температурний коефіцієнт опору, Магнітоопір, Намагніченість.